Published in final edited form as:
Biomacromolecules. 2009 June 8; 10(6): 1374–1380. doi:10.1021/bm801396e.

Fast Dynamics of Semiflexible Chain Networks of Self-Assembled Peptides

Monica C. Branco[a], **Florian Nettesheim**[a,c], **Joel P. Schneider**[b], and **Norman J. Wagner**[a,*]

[a]Department of Chemical Engineering, University of Delaware, Newark, DE 19716, USA

[b]Department of Chemistry and Biochemistry, University of Delaware, Newark, DE 19716, USA

Abstract

We present the first neutron spin echo (NSE) measurements of self-assembling peptide hydrogel networks to study the fibril dynamics on the nanometer and nanosecond length and time scales. MAX1 and MAX8 are synthetic β-hairpin peptides that undergo triggered self assembly at the nanoscale to form a physically crosslinked network of fibrils with a defined cross-section. When subjected to physiological pH and ionic strength (pH 7.4, 150 mM NaCl), the soluble peptides fold into a β-hairpin, and subsequently, self-assemble to form a structurally rigid hydrogel stabilized by non-covalent crosslinks. The sequence of MAX8 is identical to MAX1 with the exception of one single amino acid substitution which reduces the net charge on the peptide. As a result, faster folding and self assembly kinetics are observed for MAX8 at the same peptide concentration and identical buffer conditions, and gels with a larger storage modulus are formed. NSE measurements of the peptide hydrogels demonstrate that the self-assembled peptide fibrils can be described as semiflexible chains on nano-length and time scales. Alteration of the peptide sequence affected the nanoscale dynamics of the hydrogels, but not to an extent comparable to the large difference observed in the bulk viscoelasticity. Small angle neutron scattering (SANS) of the hydrogels reveals increased scattering for MAX8 at low wavevectors, an indication of a heterogeneous network with a tighter mesh size. Therefore, we conjecture that the difference in elastic modulus arises from differences in assembly kinetics that result in increased fibrillar branching and physical crosslinks, rather than a change in the fibril nanostructure or persistence length.

Keywords

peptide; self-assembly; viscoelasticity; neutron spin echo; small angle neutron scattering; hydrogel; semiflexible network

Introduction

The cytoskeleton within cells is comprised of several self-assembled biopolymers, which include actin, microtubules, and intermediate filaments. Networks of these protein filaments maintain cell shape, provide mechanical stability, and aid cell migration. To better understand how these systems function *in vivo*, the structure and dynamics of these biopolymers has been

*Corresponding Author: wagnernj@udel.edu.
[c]Current address: DuPont Central Research and Development, Wilmington, DE USA

Supporting Information Available. Analytical RP-HPLC chromatograms of the purified peptides and their corresponding mass spectral data, oscillatory shear rheology of 1.0wt% and 1.5wt% MAX1 and MAX8 at pH 7.4, 150 mM NaCl and 25°C, plots of the normalized intermediate scattering functions for β = 0.5, 2/3, and 1, plots of the intermediate scattering functions to determine β, curves of the NSE relaxation rates as a function of q for each peptide concentration with fits for D_G (Equation 2), and a table of SANS model fitted parameters. This material is available free of charge via the Internet at http://pubs.acs.org.

extensively studied *in vitro*.[1-12] Rheological and spectroscopy techniques show that these polymer chains are semiflexible and form networks with unique viscoelastic properties, such as high storage moduli at low monomer concentrations[6], significant strain hardening at low strain[4, 12], and a negative normal force upon shear[2]. Recently, synthetic polymers have been developed with similar semiflexible characteristics. One example is a synthetic β-hairpin peptide analogue, termed MAX1, which undergoes triggered self assembly at the nanoscale to form a physically crosslinked network of fibrils with a defined cross-section.[13-16] The resulting hydrogels display bulk viscoelastic behavior similar to networks of naturally occurring semiflexible biopolymers.[14]

The primary sequence of MAX1 consists of a total of 20 amino acids with alternating valine (V) and lysine (K) residues on two β-strands.[13-16] These strands are centrally connected by a tetrapeptide (-V^{D}PPT-) sequence that has a high propensity to adopt type II′ β-turn configuration (Figure 1A). In pH 7.4 aqueous solutions at low ionic strength, these peptides are designed to remain freely soluble and unfolded due to electrostatic repulsions between the positively charged lysine side chains (Figure 1B). When a physiologically relevant salt concentration is introduced (150 mM NaCl), the electrostatic repulsions between the lysine side chains are screened and the peptide folds into a β-hairpin structure, stabilized by intramolecular hydrogen bonds.[13, 14] When folded, the hairpin exhibits facial amphiphilicity with one face containing hydrophilic lysine residues and the other face comprised of hydrophobic valines. The valine-rich face undergoes hydrophobic collapse, driving the self-assembly of the folded hairpins into fibrils, which are further stabilized by intermolecular hydrogen bonding.[17] These two events, folding and self-assembly, although discussed as separate events, are most likely occurring concurrently. The resultant fibrils are essentially irreversibly assembled, such that their structure is path dependent. Transmission electron microscopy (TEM), small angle neutron scattering (SANS), and rheology demonstrate that the resultant, rigid networks of the semiflexible fibrils are composed of a bilayer of hairpins with a cross-sectional diameter of 3 nm, corresponding to the width of a folded peptide (Figure 1C). The fibrils are connected by non-covalent, interfibrillar junctions and entanglements.[13, 14, 16] Imperfections in the self assembly mechanism, in which one hairpin is rotated relative to another hairpin in the bilayer, gives rise to interfibril branching (Figure 1B).

MAX8 is an alternate peptide sequence derived from MAX1, in which a lysine at position 15 on the hydrophilic face is replaced with a glutamic acid residue (Figure 1A).[18, 19] This substitution reduces the positive charge on this face, which reduces the electrostatic repulsion between adjacent peptides in the fibril. Hence, faster folding and self-assembly kinetics are observed for MAX8 at the same peptide concentrations and buffer conditions. Rheo-kinetic studies of the hydrogel formation also show that these faster kinetics lead to a more rigid gel at the same concentration of peptide as MAX1.[19] TEM of the two systems, MAX1 and MAX8, indicates that the peptides have equivalent fibril widths and comparable physical structure on the ~1-100 nm scale.[18] This is further verified by SANS measurements, which yield fibril diameters of about 3 nm for both peptides.[20] Therefore, the increased rigidity for MAX8 folded at the same peptide concentration, temperature, and buffer is hypothesized to be a consequence of structural differences on length scales of the mesh size, either in terms of the topology of the network (i.e., more branch points due to imperfections in the self-assembled bilayer of the fibrils in MAX8) or in the compactness of the bilayer (i.e., higher bending constant).

Neutron spin echo (NSE) spectroscopy has been successfully used to determine the dynamics of self-assembled micellar systems, such as microemulsions and lamellar phases, on length and time scales comparable to segmental and center of mass motion.[21-23] The method is also well established for probing polymer dynamics.[24-27] Dynamic light scattering (DLS) has been previously utilized to observe the dynamics of polymers and self assembled peptides[28-30]; however, NSE is able to probe shorter time scales, 10^{-11} to 10^{-7} seconds, and shorter length

scales, 0.5 to 50 nm, at a larger momentum transfer.[24-26, 31, 32] Also, NSE can probe more concentrated solutions and gels, since multiple scattering effects are reduced in this method.[32] A rigorous analysis of the local dynamics of bilayer systems was presented by Monkenbusch et al. with NSE,[33] based on the theory for bilayer dynamics by Granek et al.[34] Similarly, wormlike micelles have been studied by NSE using a similar approach and the semiflexible chain model of Zilman and Granek.[35] However, the method has not, to date, been used to study the dynamics of self-assembled peptides.

Based on the bulk viscoelastic measurements, it is anticipated that the segmental dynamics of the peptide hydrogels will be comparable to that of the self-assembled worm-like surfactants recently studied.[23, 36] Theory predicts that the dynamic structure factor for the fast dynamics of semiflexible chains and macromolecules relaxes as a stretched exponential with a scaling exponent of $\beta = ¾$.[23, 34, 35, 37, 38] Deviations from these predictions could point to the existence of defects in the peptide fibrillar structure, such as crosslinks, which would manifest in a scaling closer to translational diffusion. Furthermore, analysis of the intermediate scattering function using the semiflexible chain model will allow for an estimation of the segmental diffusion coefficient for both peptide sequences.

Here, we report the first NSE measurements of self-assembling peptide hydrogel networks to study their dynamics on the nanometer and nanosecond length and time scales, which are outside the limits of common DLS measurements. These measurements are designed to explore whether these self-assembled peptide fibrils can be described by the theory of semiflexible chains on length scales smaller than the mesh size of the fibril network.[14] In addition, these studies will ascertain if the substitution of the lysine at position 15 with a glutamic acid affects the nanoscale dynamics. Specifically, this analysis was performed to determine whether the observed difference in viscoelastic behavior is due to a difference in nanoscale fibril rigidity. We follow the procedures and theoretical analysis defined in recent work on self-assembled worm-like surfactants based on the theory of Zilman and Granek.[23]

Materials and Methods

Materials

Bis-tris propane (BTP) and sodium chloride (NaCl) were purchased from Sigma-Aldrich. D_2O was purchased from Fischer Scientific. MAX1 and MAX8 peptides were synthesized and prepared according to a previously published protocol.[18, 19]

Rheological Experiments

MAX1 and MAX8 hydrogels of 1.0 and 1.5 wt% were prepared using a pH 7.4, 50 mM BTP buffer with a salt concentration of 150 mM NaCl. Oscillatory rheology experiments were performed on a Paar Physica MCR 500 rheometer using 25 mm diameter stainless steel parallel plate geometry. A dynamic time sweep was initially performed to measure the onset of viscoelasticity of the hydrogels directly prepared in the rheometer. Experiments were done at a frequency of 6 rad/sec and 0.2% strain as a function of time for one hour at 25°C. A dynamic frequency sweep (0.1 to 100 rad/sec at constant 0.2% strain) was then performed, followed by a dynamic strain sweep (0.1 to 1000% strain at constant 6 rad/sec) for all samples (see Supporting Information).

Neutron Scattering Experiments

For the NSE and SANS experiments, samples were prepared as described above for the rheological experiment, except in D_2O. D_2O was used to ensure maximum contrast and minimize incoherent background. Hydrogel samples were prepared 24 hrs prior to the scattering experiment directly within the sample cell and maintained at 25°C at all times. NSE

was performed at the NG-5 beamline at the NCNR at NIST in Gaithersburg, MD, with $\lambda = 8$ Å, $0.5 \leq q \leq 1.25$ nm^{-1}, and $0.5 \leq \tau \leq 40$ ns. SANS was performed at the NG-7 beamline at the NCNR at NIST in Gaithersburg, MD with $\lambda = 6$ Å with a velocity selector having a wavelength spread of 0.11 at sample-to-detector distances of 1 m, 4.5 m, and 12 m. Standard procedures for NSE and SANS data acquisition and analysis were followed.[16, 20, 23]

Results and Discussion

Bulk Rheological Properties of Hydrogels

Figure 2 shows a dynamic frequency sweep for the 1.0 and 1.5 wt% MAX1 and MAX8 hydrogels. Values for the gels' plateau storage moduli, which are evaluated at the frequency where G" is a local minimum, are summarized in Table 1. All peptide hydrogels display comparatively large storage moduli given the low peptide concentrations. Previous studies of the peptide hydrogels show a power law scaling of the moduli with peptide concentration[14, 19, 20, 39]; MAX1 hydrogels scale as $G' \sim c^{2.5}$ and MAX8 hydrogels scale as $G' \sim c^{1.8}$. However, plateau storage moduli of the MAX8 hydrogels are significantly greater than those for the MAX1 hydrogels at the same peptide concentration. For example, the 1 wt% hydrogels of MAX1 and MAX8 have G' values of 200 Pa and 1700 Pa, respectively. All samples have storage moduli that are at least an order of magnitude greater than the loss moduli and were nearly independent of the frequency over the measured range (0.1 to 100 rad/sec). No crossover point was observed between G' and G" at the lower frequencies. These mechanical properties clearly indicate that the MAX1 and MAX8 gels are rigid, physically crosslinked elastic materials with rheological properties at these frequencies similar to natural, semiflexible, crosslinked networks, as previously observed.[6, 14]

Determination of Nanoscale Fibrillar Dynamics

The normalized intermediate scattering function *I(q,t)/I(q,0)* obtained from the NSE measurements is shown in Figure 3 for the 1.0 wt% MAX1 (A) and MAX8 (B). A non-decaying, elastic, component was not observed for the samples in these NSE experiments, although it is expected since the materials are elastic gels. However, the time scale accessible for the NSE experiment may be too short to observe this plateau.

The normalized intermediate scattering functions for all samples were fit using Equation 1:

$$\frac{I(q,t)}{I(q,0)} = \exp\left(-(\Gamma(q)t)^{\beta}\right) \quad (1)$$

where *I(q,0)* is the intermediate scattering function at a wavevector *q* and time 0, *I(q,t)* is the intermediate scattering function at a wavevector *q* and time *t*, $\Gamma(q)$ is the relaxation rate, and β is the stretched exponent. The value of β reflects the chain topology, ranging from 0.5 for a Rouse chain, 2/3 for a Zimm chain, and 1 for a freely diffusing, Gaussian polymer. For semiflexible chains, β is ¾. At the low wavevectors observed with NSE, $0.2 < q < 1.25$ nm^{-1}, which correspond to length scales below 30 nm, the dynamics observed by NSE arise from the individual fibrils, in particular, the folded peptides that comprise the fibrils. Since all the peptides are of the same dimensions, there should be little heterogeneity in the dynamics at these length scales. At larger length scales, where entanglements and branch points are prominent, the dynamics may be influenced by heterogeneities in the distribution of crosslinks. Figure 4a shows that the intermediate scattering functions for the peptides follow the semiflexible chain model with an average fitted β value of 0.74 ± 0.8 for all peptide gels (see Supporting Information for the other model fits and the intermediate scattering function fits

for β). The value of β = ¾ is held fixed and Γ(*q*), the relaxation rate, is then determined from fitting the measurements to Equation 1.

The segmental diffusion coefficient, D_G, is given by Equation 2:

$$\Gamma(q)=D_G q^{2/\beta} \tag{2}$$

This parameter describes the rate of mobility and flexibility of the individual fibrils in terms of bending vibrational motion. The relaxation rates for the 1.0 and 1.5 wt% MAX1 and MAX8 hydrogels are plotted in Figure 4b as a function of wavevector to determine D_G. Over most of the range of scattered wavector (q) explored, Γ(q) follows the 8/3 power law that is predicted for semiflexible chains. Deviations are observed at lower q values less than 0.3 nm^{-1}, which are typical and attributed largely to experimental difficulties in capturing sufficient decay at these low q values.[23] This wavevector also corresponds to a length scale of ~2π/q = 20 nm, which is approaching the mesh size of the networks[14, 23]. These data are excluded from the fits to determine D_G.

The segmental diffusion coefficients, D_G, were obtained by non-linear regression using Equation 2 and are reported in Table 1 for each sample. Individual fits of D_G for 1.0 and 1.5% MAX1 and MAX8 are provided in the Supporting Information. The diffusion coefficients are independent of peptide concentration for both peptide sequences, which is expected because the peptide concentrations are very low. More importantly, there is a difference between D_G for MAX1 and MAX8. MAX1 has a segmental diffusion coefficient of 1.4×10^{-2} ($nm^{8/3}ns^{-1}$) compared to 0.9×10^{-2} ($nm^{8/3}ns^{-1}$) for MAX8. This indicates that the fibrils in the MAX1 network are more mobile on this length scale.

According to the theory of Zilman and Granek, the segmental diffusion coefficient is function of three main parameters: the viscosity (μ) of the surrounding medium (in this case, the viscosity of water is assumed; μ ~ 0.001 Pa·s), the bending modulus (κ) of the individual semiflexible chains, and the lower cutoff length (a) for fibrillar diffusive motion:

$$D_G=0.0056 \ln\left(\frac{\kappa \ln\left(\frac{L_c}{a\pi}\right) t}{4\pi\mu a^4}\right)(k_b T)^{4/3}\kappa^{-1/3}\mu^{-1} \tag{3}$$

where L_c is the contour length and t is an averaged time for the NSE experimental time window of 0.5 – 40 ns.[35] For the NSE experiments, all samples were subjected to the same buffer condition. Although there may be local viscosity effects, it can be assumed that the viscosity term is the same for both peptide networks. Also, the peptide β-hairpins and the corresponding fibrils have similar dimensions in contour lengths and diameters as observed with TEM.[14, 18, 20] Therefore, according to Equation 3, this indicates that MAX1 and MAX8 fibrils may have differences either in their bending moduli or the lower cutoff length.

The bending constant, κ, is related to the persistence length of the fibrils by the relationship, $\kappa \sim l_p kT$. The persistence length of the self assembled fibrils of MAX1 hydrogels prepared at pH 7.4, 150 mM NaCl, and 25°C was previously estimated from rheological experiments to be 55 nm.[14] The NSE measurements are unable to probe the dynamics at length scales above 20 nm due to scattering on the order of the mesh size. Therefore, it is not possible to measure differences in dynamics on length scales above this value, such as persistence lengths.

However, the differences that are observed with NSE are at length scales below 20 nm, which may be more likely attributed to the parameter *a*, the lower cutoff length.

Assuming the persistence length of the two networks are approximately the same (55 nm) as previously calculated[14], Equation 3 can then be used to estimate *a* for these peptide networks. We find *a* is approximately 3.0 ± 0.2 nm for a D_G value of 1.4×10^{-2} $nm^{8/3}ns^{-1}$ (MAX1) and 3.6 ± 0.2 nm for 0.9×10^{-2} $nm^{8/3}ns^{-1}$ (MAX8). The contour length is taken to be ~ 1000 nm for the peptide fibrils; a sensitivity analysis for a range of values for L_c demonstrates that the resultant calculated values of *a* are not significantly different.[35]

This parameter *a* is undefined in molecular terms but can be interpreted as a length scale corresponding to a given number of hairpin units along the length of the fibril that are inflexible due to strong interactions between the peptides. The calculated values of *a* for MAX1 and MAX8 correspond to the width of about 6 hairpins (width of individual hairpin = 0.5 nm, Figure 1) and about 7 hairpins, respectively, lined up along the fibril axis. One can envision that the fibril chains of MAX1, for example, is composed of these rigid units stacked one after the other, yielding a persistence length of 55 nm. As the electrostatic interactions controlling self-assembly along the hydrophilic face differ between the peptides, it is reasonable to expect the value of *a* to differ as well. On the hydrophilic face of the MAX8 peptide is a negatively charged glutamic acid across from a positively charged lysine residue. This cross-strand salt bridge can propagate along the length of fibril, forming strong intermolecular interactions between hairpins, increasing the rigidity along the fibril, giving rise to a larger cut-off length and lower segmental diffusion coefficient, as observed.

Effect of Nanoscale Structure on Material Properties

The NSE data shows that there are differences in the flexibility of the individual fibrils that comprise each given peptide hydrogel that are consistent with the change in peptide sequence. However, this difference, although significant, is relatively small in magnitude and therefore, does not explain the order of magnitude higher storage modulus observed for MAX8 as compared to MAX1 under identical peptide concentration and buffer conditions. According to Mackintosh et al.[6], for densely cross-linked gels of semiflexible polymers, a scaling theory predicts the plateau modulus as

$$G'_p = \frac{\kappa^2}{kT}\xi^{-5} \tag{4}$$

where ξ is the mesh size or the average spacing between chains, comparable to the entanglement length. Therefore, since the bending moduli of the fibril can be assumed to be nearly equivalent for the two peptide sequences, the difference in mechanical rigidity of the hydrogels can be attributed to differences in the number of crosslinked junctions between the chains, which results in different characteristic mesh sizes.

A closer look at SANS data, Figure 5, for 1.0 and 1.5 wt% MAX1 and MAX8[20] under these buffer conditions supports this assessment. At high q values corresponding to the length scales of the individual fibril widths, the scattering intensities of MAX1 and MAX8 overlap. SANS scattering intensities for MAX1 and MAX8 were first fit to the equation, I(q) = P(q) S(q), where S(q), the structure factor, is initially assumed to be 1. The form factor P(q) for monodisperse rigid, circular cylinders with uniform scattering length density,

$$P(q)=\frac{\phi}{V_{cyl}}\int_0^{\frac{\pi}{2}} f^2(q,\alpha)\sin\alpha d\alpha \tag{5}$$

where ϕ is the volume fraction of peptide in the gel, V_{cyl} is the volume of the cylindrical fibrils ($V_{cyl} = \pi r^2 L$, where r is the radius of the cylinder and L is the length of the cylinder), α is the angle between the cylinder axis and the scattering vector q, and

$$f(q,\alpha)=2(\rho_{cyl}-\rho_{solv})V_{cyl}\frac{\sin(qH\cos\alpha)}{qH\cos\alpha}\frac{J_1(qr\sin\alpha)}{qr\sin\alpha} \tag{6}$$

where ρ is the scattering contrast, H is L/2, and J_1 is the first order Bessel function. The spectra for the peptide hydrogels can be reasonably fit by this form factor at high wavevectors, yielding a fibril radius of 1.5 ± 0.1 nm, which is consistent with the self assembly mechanism outlined in Figure 1 and TEM data.[18] The spectra for MAX1 at both peptide concentrations can be reasonably fit by this form factor, as shown. MAX8, on the other hand, shows a strong increase in scattering at low wavevectors as a deviation from the form factor for a rigid cylinder.

At low wavevectors, i.e., larger distances, the cylindrical rodlike fibrils interact with one another through entanglements and branch points, forming a network that is heterogeneous with densely crosslinked regions and poorly crosslinked regions.[27, 40-42] Microrheology and cryo-TEM of the gelation process of these gels describe the resultant network as a fractal gel formed from the percolation and growth of fibrillar clusters.[39, 43, 44] The clusters which are comprised of branched fibrils, give rise to the densely crosslinked fractal regions. The poorly crosslinked areas are the spaces between the clusters, which are connected through interactions between dangling ends and extended fibrils. Therefore, the scattering intensity at these low wavevectors should not be represented by a simple rigid cylindrical model and thus, the SANS data for MAX1 and MAX8 were fit to a structure fractal model with the scattering intensity I (q) = P(q) S(q). In this fractal model, the form factor is calculated for spherical particles:

$$P(q)=\phi V_p(\rho_{cyl}-\rho_{solv})^2 F(qR_0)^2 \tag{7}$$

where R_0 is the radius of the particle with a $V_p = 4/3\pi R_0^3$ and

$$F(x)=\frac{3[\sin x - x\cos x]}{x^3} \tag{8}$$

With this model, the peptide fibrils are approximated as an array of spherical building blocks with radius R_0 that assemble along a central axis. The fibrils then aggregate to form fractal-like clusters with a correlation length, ξ, corresponding to the average cluster size and a self-similarity dimension of D_f. The effective structure factor of these clusters can be calculated by Equation 9.[40]

$$S(q)=1+\frac{\sin\left[(D_f-1)\tan^{-1}(q\xi)\right]}{(qR_0)^{D_f}}\frac{D_f\Gamma(D_f-1)}{[1+1/(q^2\xi^2)]^{(D_f-1)/2}} \tag{9}$$

S(q) is equal to 1 for a fractal dimension of 1 and the scattering intensity is only a function of the form factor. A fractal dimension of 2 simplifies the equation to the Ornstein-Zernike, or Lorentzian, form of S(q).[40, 41] Fitting the data for the MAX1 gels yields a fractal dimension of 1.2 with cluster correlation sizes of 1250 nm for the 1wt% gels and 700 nm for the 1.5% gels (see Supporting Information for table of fitted parameters). The MAX8 gels have a larger fractal dimension of 1.6 and smaller cluster sizes of 560 nm for the 1 wt% gels and 380 nm for the 1.5 wt%, Figure 5. The fractal model also yields an average radius of 1.9 ± 0.1 nm for the peptide fibrillar gels, in agreement with the cylindrical form factor fit and previous TEM data.[18]

The fractal model cannot accurately fit the low q region, in particular for the 1.5 wt% MAX8 gels. This indicates that the gels can only be described by a fractal dimension within a distinct spatial range, typically one decade of length scales, and therefore, the model breaks down at some scale in the real experiment.[40] However, the fits do show that MAX8 has a higher fractal dimension, which can indicate the presence of a more heterogeneous, tighter network compared to MAX1. The smaller cluster sizes observed for MAX8 indicate that there are more branching nucleation points of fibrils in the network that give rise to the increased scattering intensity. This is important because the presence of more branchpoints will then result in increased storage moduli, as observed in rheology.

The self assembling mechanism of these β-hairpin peptides can be used to rationalize how a solution of the same concentration of peptide at identical buffer, temperature, and preparation conditions can have different structural properties (Figure 1B). The peptide hairpins facially assemble to form a bilayer in which the β-strands are antiparallel and in register with each other to shield the maximum amount of the hydrophobic valine surface area from water (Figure 1C). Imperfections in this mechanism, in which one hairpin is rotated relative to another hairpin in the bilayer, can result in interfibril branching (Figure 1B). Therefore, it is expected that rapid self assembly can lead to the formation of more facial imperfections and a greater amount of interfibrillar junctions along the fibril axis. This increases the number of overall crosslinks in the network, which results in an increase in the mechanical rigidity and a decrease in the network mesh size.[13, 15-18] Also, the higher fractal dimension of the MAX8 gels calculated from the SANS data is consistent with systems that have fast growth kinetics and result in more heterogeneous networks, rather than systems with linear growth of fibrils. Therefore, by reducing the electrostatic repulsions along the hydrophilic face, MAX8 not only folds and self assembles faster than MAX1 under identical conditions, but hydrogels from MAX8 have a higher propensity to have more interfibrillar imperfections that lead to increased bulk rigidity and more heterogeneities in network structure. Furthermore, the increased steric hindrances imposed by the presence of more branches can further limit the mobility of the MAX8 fibrils, resulting in a lower value for the segmental diffusion coefficient as compared to the MAX1 network.[45]

Conclusions

MAX1 and MAX8 are synthetic β-hairpin peptides that undergo triggered self assembly at the nanoscale to form physically crosslinked hydrogels with great potential for both drug delivery and tissue engineering applications. Using peptides as building blocks for the assembly of hydrogels allows one to make sequence specific modifications at the molecular level that ultimately influence the bulk properties of the self-assembled network. For example, the single amino acid substitution of MAX1, affording MAX8, resulted in faster folding and self assembly kinetics at the same peptide concentration and identical buffer conditions, and gels with higher storage moduli are formed. Neutron spin echo (NSE) measurements demonstrate that these peptide hydrogels can be described as semiflexible chains at the nanoscale, and that differences in peptide sequence are reflected in the nanoscale dynamics. Complementary small angle

neutron scattering (SANS) measurements of the networks show that the large difference in the bulk elasticity is a result of increased fibrillar branching and physical crosslinking that arises from the effect of peptide sequence on the rate of assembly. Ultimately, these neutron scattering techniques allowed us to determine the full impact that molecular changes had on the dynamic and structural properties of the self assembled fibrils. It is only by understanding material properties from the nanoscale up to the macroscale that better and specific design of the self-assembling peptide materials can be achieved, allowing for the controlled design of these systems for many biomaterial applications.

Supplementary Material

Refer to Web version on PubMed Central for supplementary material.

Acknowledgments

This work was prepared under 70NANB7H6178 from National Institute of Standards and Technology (NIST), U.S. Department of Commerce. The statements, findings, conclusions, and recommendations are those of the authors and do not necessarily reflect the views of NIST or the U.S. Department of Commerce. Support from the UD Center for Neutron Science is acknowledged. This work was also supported by National Institutes of Health Grant (NIH) R01 DE016386-01. We also thank Antonio Faraone (NIST-NCNR) for his assistance in performing and analyzing the NSE experiments and Matthew Helgeson and Dennis Kalman (University of Delware) for their assistance with SANS analysis.

References

1. Isambert H, Maggs AC. Macromolecules 1996;29(3):1036–1040.
2. Janmey PA, McCormick ME, Rammensee S, Leight JL, Georges PC, Mackintosh FC. Nat Mater 2007;6 (1):48–51. [PubMed: 17187066]
3. Lin YC, Koenderink GH, MacKintosh FC, Weitz DA. Macromolecules 2007;40(21):7714–7720.
4. Liu J, Koenderink GH, Kasza KE, MacKintosh FC, Weitz DA. Phys Rev Lett 2007;98(19):198304. [PubMed: 17677669]
5. Mackintosh FC, Janmey PA. Curr Opin Solid State Mater Sci 1997;2(3):350–357.
6. Mackintosh FC, Kas J, Janmey PA. Phys Rev Lett 1995;75(24):4425–4428. [PubMed: 10059905]
7. Maggs AC. Phys Rev E: Stat, Nonlinear, Soft Matter Phys 1997;55(6):7396–7400.
8. Muller O, Gaub HE, Barmann M, Sackmann E. Macromolecules 1991;24(11):3111–3120.
9. Storm C, Pastore JJ, MacKintosh FC, Lubensky TC, Janmey PA. Nature 2005;435(7039):191–194. [PubMed: 15889088]
10. Xu JY, Palmer A, Wirtz D. Macromolecules 1998;31(19):6486–6492.
11. Xu JY, Schwarz WH, Kas JA, Stossel TP, Janmey PA, Pollard TD. Biophys J 1998;74(5):2731–2740. [PubMed: 9591697]
12. Head DA, Levine AJ, MacKintosh FC. Phys Rev E: Stat, Nonlinear, Soft Matter Phys 2005;72(6): 061919.
13. Ozbas B, Kretsinger J, Rajagopal K, Schneider JP, Pochan DJ. Macromolecules 2004;37(19):7331–7337.
14. Ozbas B, Rajagopal K, Schneider JP, Pochan DJ. Phys Rev Lett 2004;93(26):268106. [PubMed: 15698028]
15. Pochan DJ, Schneider JP, Kretsinger J, Ozbas B, Rajagopal K, Haines L. J Am Chem Soc 2003;125 (39):11802–11803. [PubMed: 14505386]
16. Schneider JP, Pochan DJ, Ozbas B, Rajagopal K, Pakstis L, Kretsinger J. J Am Chem Soc 2002;124 (50):15030–15037. [PubMed: 12475347]
17. Rajagopal K, Ozbas B, Pochan DJ, Schneider JP. Eur Biophys J 2006;35(2):162–169. [PubMed: 16283291]
18. Haines-Butterick L, Rajagopal K, Branco M, Salick D, Rughani R, Pilarz M, Lamm MS, Pochan DJ, Schneider JP. Proc Natl Acad Sci U S A 2007;104(19):7791–7796. [PubMed: 17470802]

19. Branco MC, Pochan DJ, Wagner NJ, Schneider JP. Biomaterials 2009;30(7):1339–1347. [PubMed: 19100615]
20. Hule RA, Nagarkar RP, Altunbas A, Ramay HR, Branco MC, Schneider JP, Pochan DJ. Faraday Discuss 2008;139:251–264. [PubMed: 19048999]
21. Matsuoka H, Yamamoto Y, Nakano M, Endo H, Yamaoka H, Zorn R, Monkenbusch M, Richter D, Seto H, Kawabata Y, Nagao M. Langmuir 2000;16(24):9177–9185.
22. Castelletto V, Hamley IW, Yang Z, Haeussler W. J Chem Phys 2003;119(15):8158–8161.
23. Nettesheim F, Wagner NJ. Langmuir 2007;23(10):5267–5269. [PubMed: 17402760]
24. Richter, D.; Monkenbusch, M.; Arbe, A.; Colmenero, J. Neutron Spin Echo in Polymer Systems. Vol. 174. Springer-Verlag Berlin; Berlin: 2005. Neutron spin echo in polymer systems; p. 1-221.
25. Monkenbusch M, Richter D. C R Phys 2007;8(78):845–864.
26. Richter D, Fetters LJ, Huang JS, Farago B, Ewen B. J Non-Cryst Solids 1991;131-133(Part 2):604–611.
27. Koizumi S, Michael M, Dieter R, Dietmar S, Bela F. J Chem Phys 2004;121(24):12721–12731. [PubMed: 15606298]
28. Simon M, Anne-Marie H, Erik G, Pierre P. J Chem Phys 1989;91(10):6447–6454.
29. Mitsuhiro S, Masahiko O. J Chem Phys 2001;115(9):4285–4291.
30. Carrick L, Tassieri M, Waigh TA, Aggeli A, Boden N, Bell C, Fisher J, Ingham E, Evans RML. Langmuir 2005;21(9):3733–3737. [PubMed: 15835929]
31. Nystrom B, Roots J, Higgins JS, Gabrys B, Peiffer DG, Mezei F, Sarkissian B. J Polym Sci, Part C: Polym Lett 1986;24(6):273–281.
32. Luca ED, Waigh TA, Monkenbusch M, Kim JS, Jeon HS. Polymer 2007;48(14):3930–3934.
33. Monkenbusch M, Holderer O, Frielinghaus H, Byelov D, Allgaier J, Richter D. J Phys: Condens Matter 2005;17(31):S2903–S2909.
34. Granek R. J Phys II 1997;7(12):1761–1788.
35. Zilman AG, Granek R. Phys Rev Lett 1996;77(23):4788–4791. [PubMed: 10062631]
36. Seto H, Kato T, Monkenbusch M, Takeda T, Kawabata Y, Nagao M, Okuhara D, Imai M, Komura S. J Phys Chem Solids 1999;60(89):1371–1373.
37. Kroy K, Frey E. Phys Rev E: Stat, Nonlinear, Soft Matter Phys 1997;55(3):3092–3101.
38. Nyrkova IA, Semenov AN. Phys Rev E: Stat, Nonlinear, Soft Matter Phys 2007;(76):011802.
39. Veerman C, Rajagopal K, Palla CS, Pochan DJ, Schneider JP, Furst EM. Macromolecules 2006;39 (19):6608–6614.
40. Teixeira J. J Appl Crystallogr 1988;21:781–785.
41. Guo XH, Zhao NM, Chen SH, Teixeira J. Biopolymers 1990;29(2):335–346. [PubMed: 2331502]
42. Vilgis TA, Heinrich G. Macromol Theory Simul 1994;3(2):271–293.
43. Larsen TH, Furst EM. Phys Rev Lett 2008;100(14):146001. [PubMed: 18518051]
44. Yucel T, Micklitsch CM, Schneider JP, Pochan DJ. Macromolecules 2008;41(15):5763–5772. [PubMed: 19169385]
45. Ramachandran R, Beaucage G, Kulkarni AS, McFaddin D, Merrick-Mack J, Galiatsatos V. Macromolecules 2008;41(24):9802–9806.

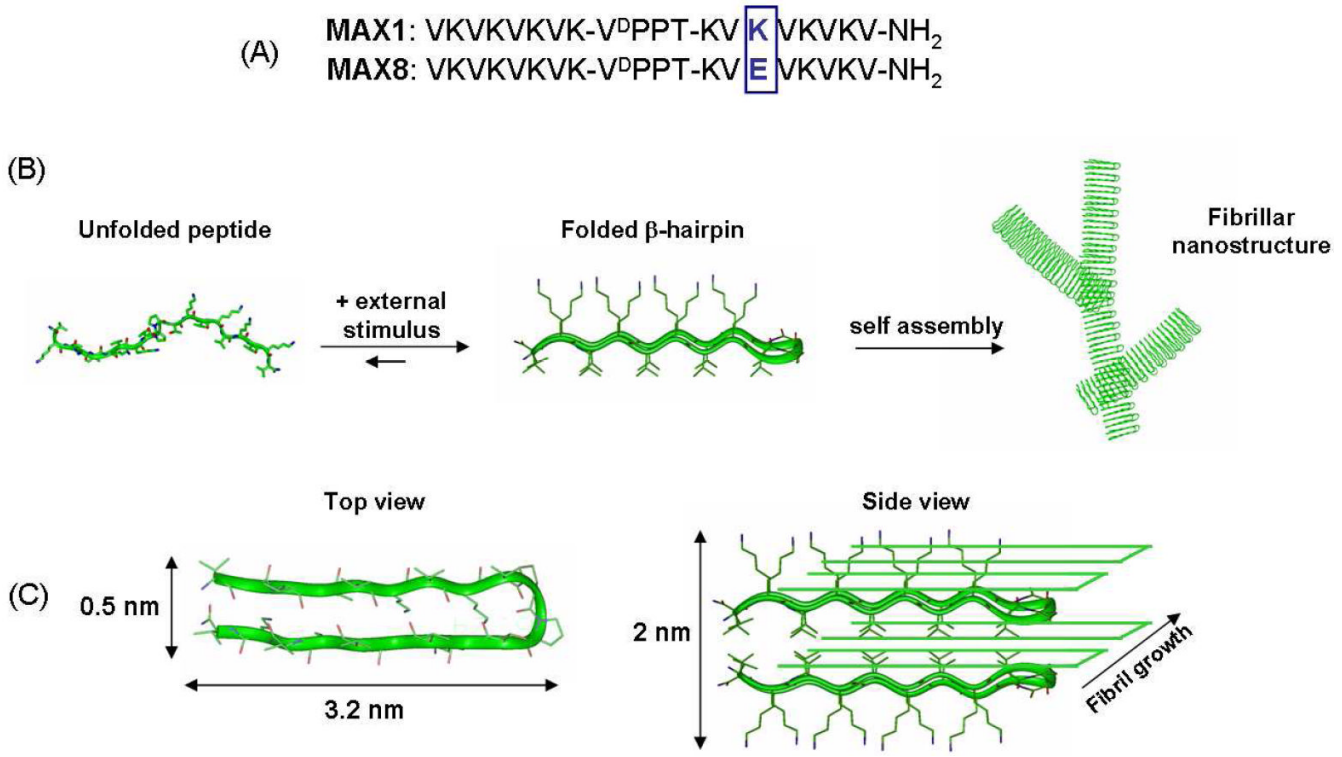

Figure 1.

(A) Peptide primary sequence for MAX1 and MAX8. (B) Proposed mechanism for the folding and self-assembly of the β-hairpin peptides. (C) Length scales of the hairpin structure and self-assembled hairpin bilayer.

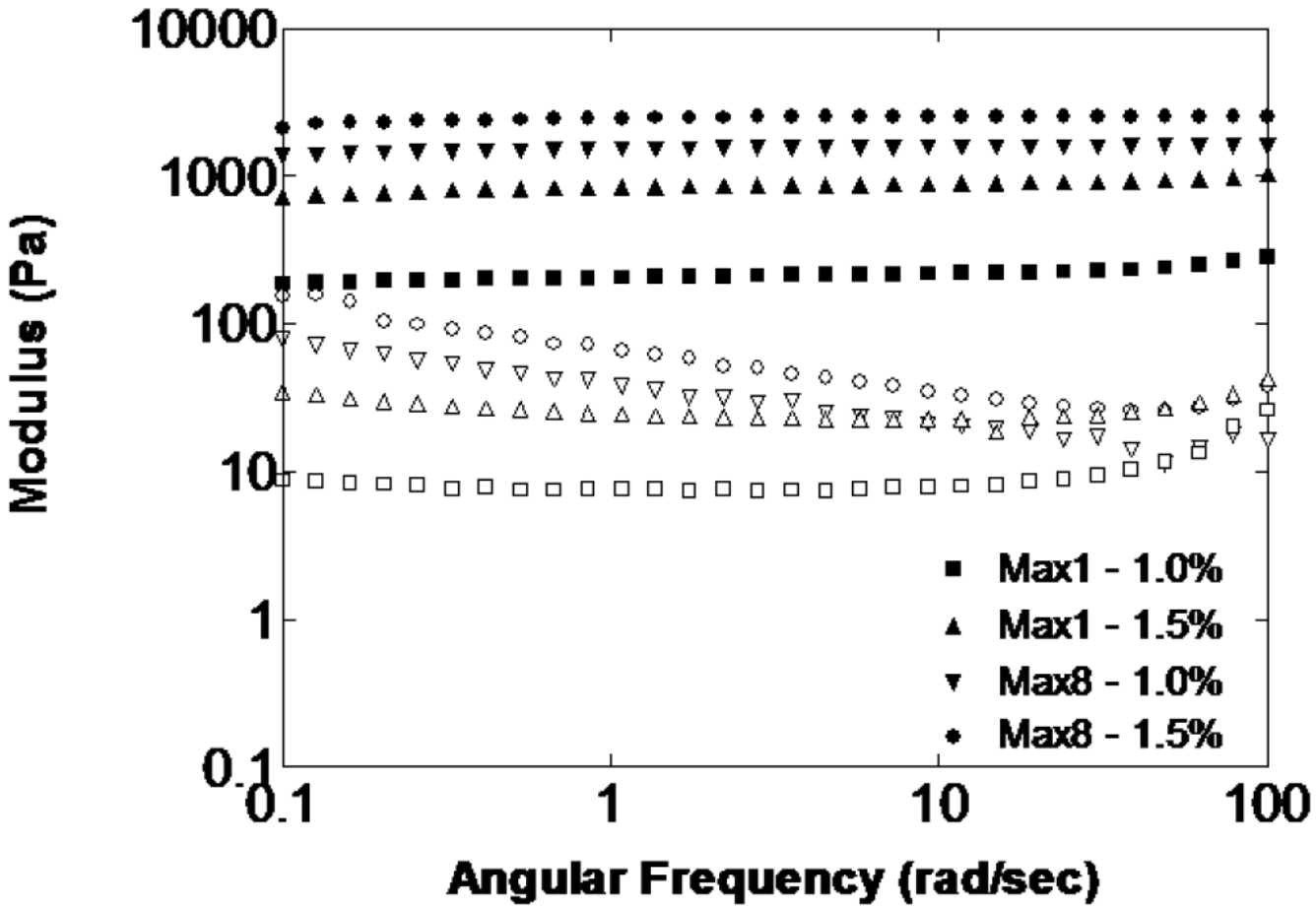

Figure 2.
Dynamic frequency sweep of 1.0 wt% and 1.5 wt% MAX1 and MAX8 hydrogels in pH 7.4, 50 mM BTP, 150 mM NaCl at 25°C (0.2 % strain). Closed symbols are the storage modulus (G') and open symbols are the loss modulus (G").

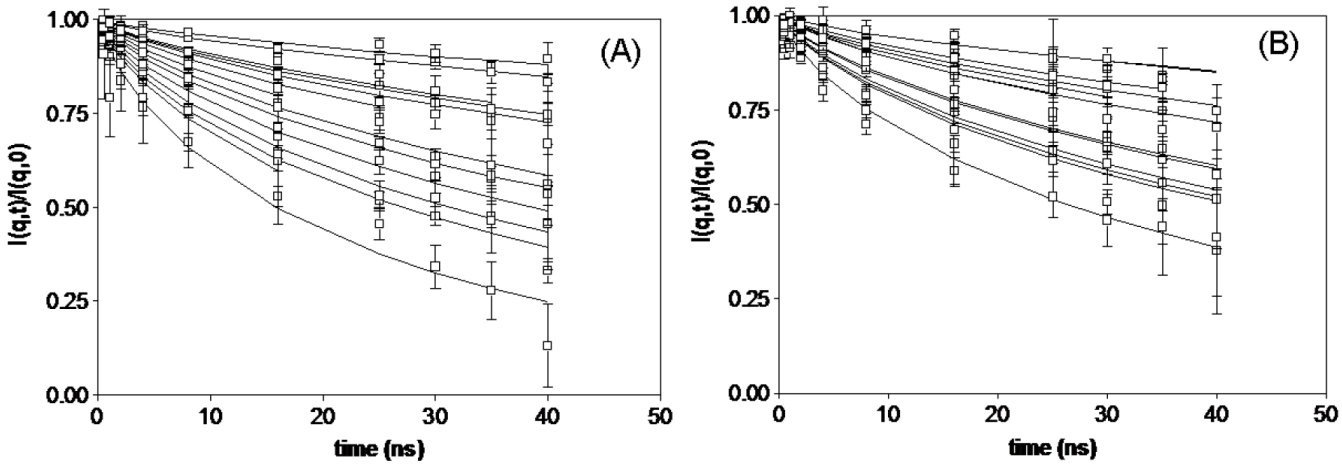

Figure 3.

Normalized intermediate scattering functions for 1 wt% MAX1 (A) and MAX8 (B) in pH 7.4, 50 mM BTP, 150 mM NaCl at 25°C at selected q values in the range of 0.2 to 1.5 nm^{-1}. Solid lines are fits to Equation 1.

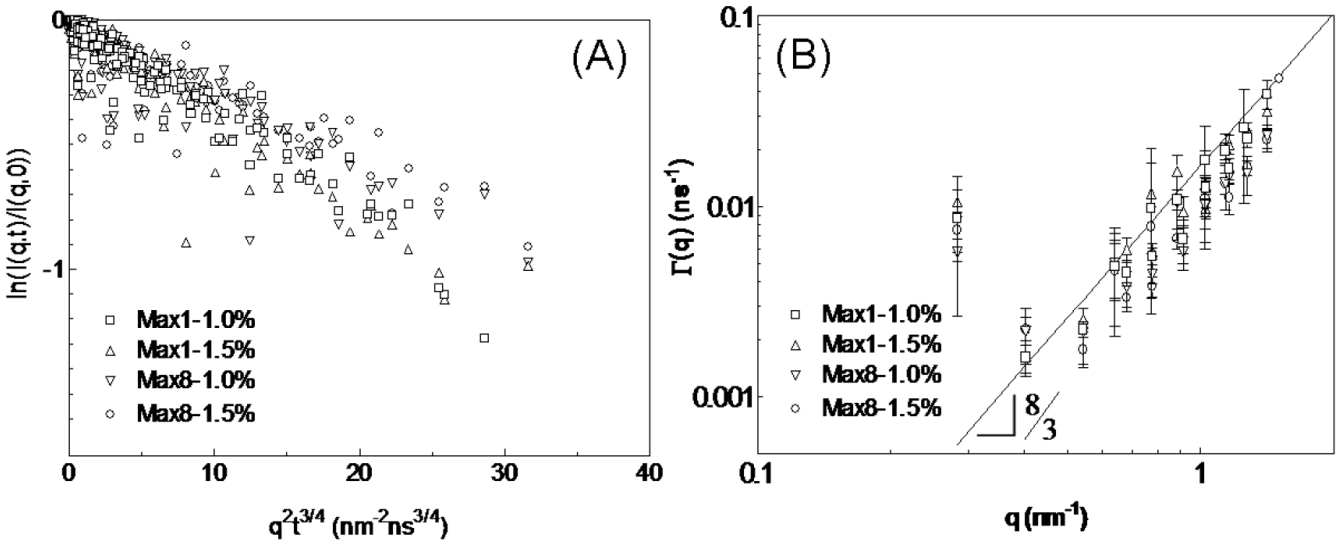

Figure 4.

(A) Normalized intermediate scattering functions plotted according to the semiflexible chain model. (B) Relaxation rate (Γ(q)) as a function of q. The solid line represents the scaling expected for the bending modes of semiflexible chains.

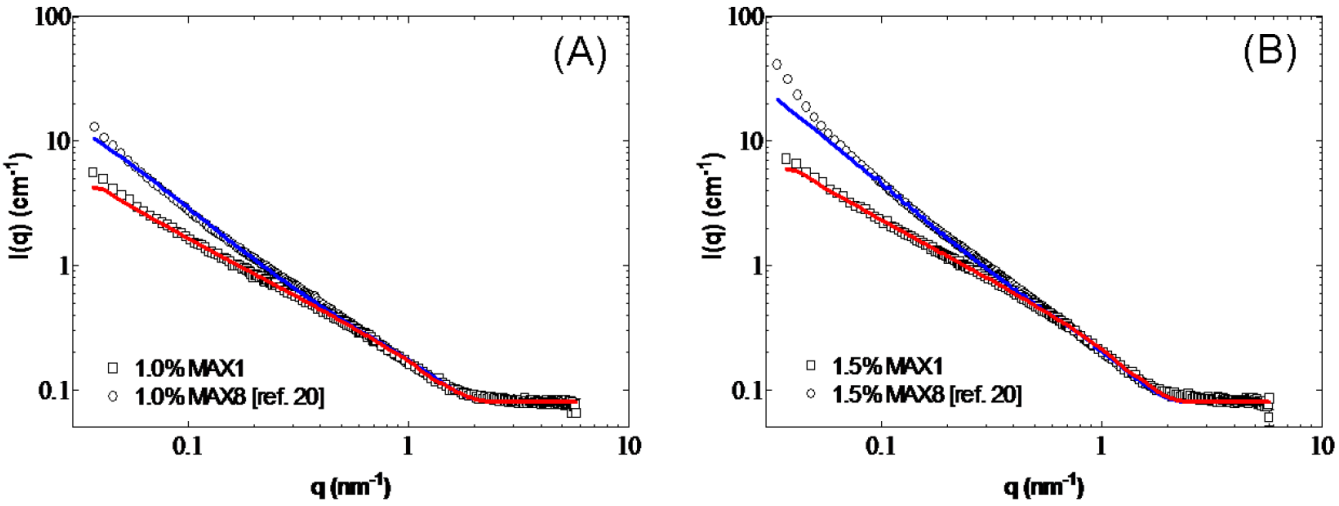

Figure 5.

SANS intensity scattering function I(q) as a function of q for (A) 1.0wt% and (B) 1.5wt% MAX1 and MAX8[20] hydrogels in pH 7.4, 50 mM BTP, 150 mM NaCl, D_2O at 25°C. Hydrogels were prepared 24 hours prior to SANS experiment. Red lines are rigid cylindrical model fit for MAX1 hydrogels and blue lines are fractal model fit for MAX8 hydrogels.

Table 1

Plateau moduli and corresponding segmental diffusion coefficients for MAX1 and MAX8 hydrogels.

Peptide	Concentration (wt%)	G'_p (Pa)	$D_g \times 10^{-2}$ ($nm^{8/3}ns^{-1}$)
MAX1	1.0	200 ± 10	1.4 ± 0.2
	1.5	880 ± 100	1.4 ± 0.2
MAX8	1.0	1700 ± 150	0.9 ± 0.1
	1.5	2500 ± 150	0.9 ± 0.1